ELECTRONIC SUPPORTING INFORMATION:
Prospects and challenges in designing photocatalytic particle suspension reactors for solar fuel processing

Swarnava Nandy*[,§], Sangram Savant*[,§], Sophia Haussener*[1]

*Laboratory of Renewable Energy Science and Engineering, Institute of Mechanical Engineering, EPFL, Station 9, 1015 Lausanne, Switzerland
[§]Equally contributing; [1]Corresponding author: sophia.haussener@epfl.ch (+41 21 69 33878)

S1. Modelling approach

Figure S1 shows the modeling flow used for the 0D model of the two-particle photocatalytic water splitting device. We calculate the current-voltage characteristic of the photocatalysts by solving the detailed balance limit for the two absorbers (with band gap of the semiconductors as input). These current-voltage characteristics is then used to balance the corresponding electrochemical loads, consisting of the concentration-dependent equilibrium potential (utilizing the Nernst equation), the concentration-dependent overpotentials of the two – MRR and OER, or HER and MOR – involved reactions (utilizing Butler-Volmer equations) and the concentration-dependent ohmic resistances of the electrolyte. This matching of the photocatalyst power curve with the electrochemical load curve for the two particles is embedded in a time-dependent loop that solves the transient diffusion transport equation with a source/sink term to account for the reaction. The surface concentration of the particle is approximated by a diffusion limiting current approach. The loop is repeated until steady state is reached, i.e. a condition where the operational current density (which is current per particle hemisphere, i.e. $i = I/((4\pi r^2)/2)$) of the two particle types are equal.

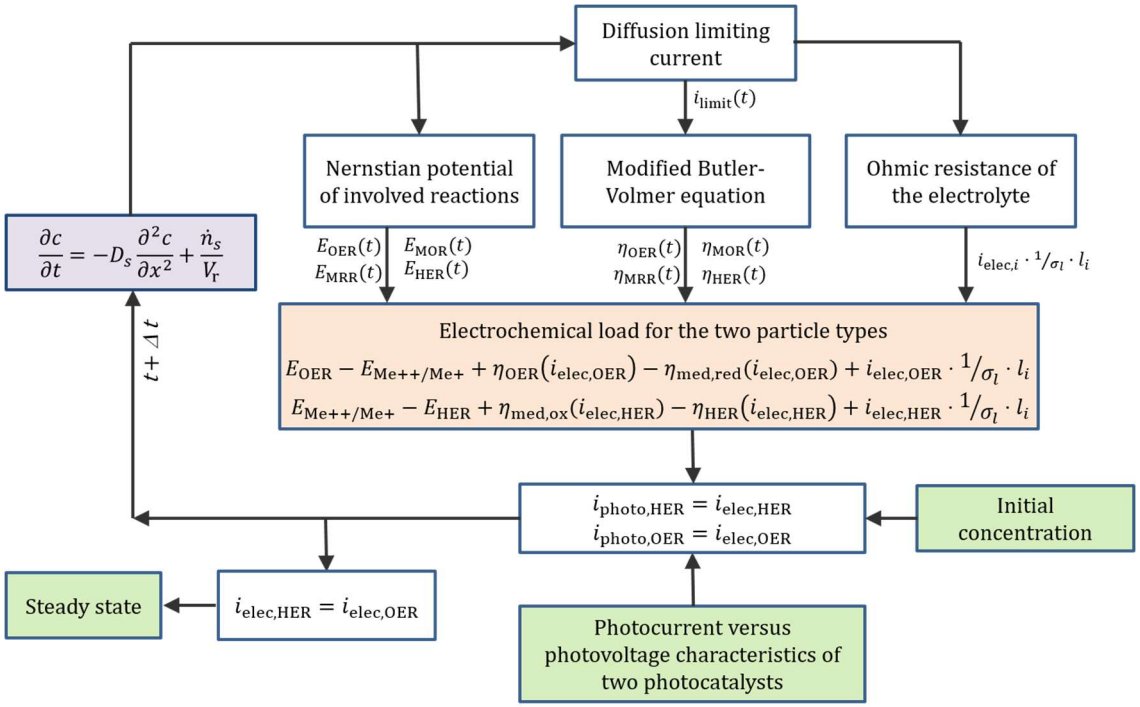

Figure S1. Modeling flow diagram of the 0D 2-particle model.

Photocatalysts performance

We treat the two semiconductor (photocatalytic component) particle types as tiny diodes[1,2]. The photocurrent as a function of the potential is calculated by solving the detailed balance limit, with the band gaps of the particle(s) as an input[3].

Nernstian Potential

The equilibrium potentials at different concentrations is calculated by the Nernst-equation

$$E = E^0 - \frac{RT}{nF}\ln\left(\frac{a_{\text{oxidation}}}{a_{\text{reduction}}}\right) \quad \text{(S1)}$$

where, E is the equilibrium potential, E^0 is the Gibbs free energy, R is the universal gas constant, T is the temperature, n is the number of participating electrons, F is the Faraday constant and a is the chemical activity of the relevant species. The activity coefficient γ relates the concentration of a reagent with its activity,

$$a_i = \gamma_i \frac{c_i}{c_i^{\theta}} \quad \text{(S2)}$$

where c_i is concentration of species i and c_i^{θ} is standard amount concentration. For an ideal dilute solution, γ_i is equal to one, thus we replace the chemical activity ratio by the concentration ratio. E^0 is 1.229 V vs SHE for OER, 0 V vs SHE for HER, and varied for MRR and MOR (where $E^0_{MRR} = -E^0_{MOR}$). For Fe^{3+}/Fe^{2+} mediator, E^0 is 0.77 V vs SHE.

Butler-Volmer equation

The electrochemical kinetics is described by an adapted Butler-Volmer expression. The Butler-Volmer expression is given by:

$$i = i_0\left[e^{\left(\frac{\alpha_a F}{RT}\eta\right)} - e^{\left(\frac{-\alpha_c F}{RT}\eta\right)}\right] \quad \text{(S3)}$$

where i is the net current density of the reaction of interest at a certain overpotential η. i_0 is the exchange current density, and α_{a} and α_{c} are the transfer coefficients for the anodic and the cathodic reaction, respectively. During the reaction ions have to be transported from the bulk to the electrode surface by diffusion, convection and migration. Without a current flowing, the concentration at the surface, c^{s}, is equal to the bulk concentration, c^0. With a current flowing, the reactant ion concentration depletes. This local depletion influences the reaction rate and can be taken into account by a concentration ratio c^{s}/c^0 for the reduced and the oxidized species, respectively. Note that the concentration terms are time-dependent to include the transient nature of the problem.

$$i(t) = i_{0,j}\left[\frac{c^{\text{s}}(t)}{c^0(t)}\bigg|_{\text{red}} \text{e}^{\left(\frac{\alpha_{\text{a},j}F}{RT}\eta\right)} - \frac{c^{\text{s}}(t)}{c^0(t)}\bigg|_{\text{ox}} \text{e}^{\left(\frac{-\alpha_{\text{c},j}F}{RT}\eta\right)}\right] \quad \text{(S4)}$$

where j indicates the four reactions (OER, HER, MRR, or MOR).

In most cases the surface concentration is not known. Therefore, the concentration ratio is estimated based on a measurable diffusion limiting current density, i_{limit}

$$i_{\mathrm{limit}} = n \cdot F \cdot D \cdot \frac{c^0}{\delta} \tag{S5}$$

The concentration ratio $\frac{c^s}{c^0}$ can then be replaced by the following expression (note again the time-dependent concentration terms as they account for mass transport limitations of the mediator species, resulting from their transport across the two chambers and the membrane[4]):

$$\frac{c^s(t)}{c^0(t)} = 1 - \frac{i(t)}{i_{\mathrm{limit}}(t)} \tag{S6}$$

where i_{limit} is the diffusion limiting current, *F* is Faraday constant, *D* is the diffusion coefficient of the concerned species, and δ is the diffusion layer thickness (which was chosen to be 5 x 10^{-6} m [4–6], a value calculated for a moderately stirred solution). We assume that the diffusion layer is much thinner than the radius of the sphere.

We then replace this concentration ratio with the time dependent diffusion limiting current in the Butler-Volmer equation,

$$i(t) = i_{0,j}\left[\left(1 - \frac{i}{i_{\mathrm{limit}}^{\mathrm{red}}(t)}\right)e^{\left(\frac{\alpha_{\mathrm{a},j}F}{RT}\eta\right)} - \left(1 - \frac{i}{i_{\mathrm{limit}}^{\mathrm{ox}}(t)}\right)e^{\left(\frac{-\alpha_{\mathrm{c},j}F}{RT}\eta\right)}\right] \tag{S7}$$

Ohmic losses

The conductivity of the electrolyte, σ_l, is calculated as follows:

$$\sigma_l = \sum_s F \cdot z_s^2 \cdot \mu_s \cdot c_s \tag{S8}$$

with z the valence of the species. The mobility μ and the diffusivity are related by the Nernst-Einstein relation for charged species.

$$\mu = \frac{q \cdot D}{k \cdot T} \tag{S9}$$

where q is the elementary charge and k the Boltzman constant. The ohmic overpotential is then calculated based on the conductivity and pathway of the charge carrier (see eqs. (S14) and (S15)). The path length of the ionic transport is estimated to be roughly one particle diameter and here assumed $l_{\mathrm{i}} = 10\ \mu\mathrm{m}$.

Mass transport and diffusion

If the operation electrochemical current density, i_{elec}, is known, the species production/consumption (i.e. source/sink terms) can be calculated by Faradays law,

$$\dot{n}_s = \frac{n_s}{\Delta t} = \frac{i_{\mathrm{elec}} \cdot A}{z \cdot F} \tag{S10}$$

where n_s is the number of moles of species *s* created/consumed, A the electrode surface area (i.e. particle hemisphere) and Δt the time step. Note that the production/consumption term is not necessarily equal in

the two compartments (given i_{elec} varies during the transient phase). The transport equation with the source term is given by,

$$\frac{\partial c_s}{\partial t} = -D_s \frac{\partial^2 c_s}{\partial x^2} + \frac{\dot{n}_s}{V_\mathrm{r}} \tag{S11}$$

where V_r is control volume of one compartment (assumed 1000 µm^3) of electrolyte through which the species are diffused. We solve the transient diffusion equation numerically by a forward Euler method:

$$c_{s,r_1}(t+\Delta t) = c_{s,r_1}(t) + \frac{i_{\mathrm{elec},r_1} \cdot A \cdot \Delta t}{z \cdot F \cdot V_\mathrm{r}} - D_s \frac{A_\mathrm{mem}}{V_\mathrm{r}} \frac{c_{s,r_2}(t) - c_{s,r_1}(t)}{(t_\mathrm{mem} + V_\mathrm{r}/A_\mathrm{mem})} \Delta t \tag{S12}$$

where $c_{s,r_i}(t = t_0)$ is the initial concentration for the species *s* in compartment one or two (r_i for *i*=1,2, alternatively also OER and HER are used as subscripts, see eqs. (S14) and (S15)). The membrane surface area A_mem is assumed 100 µm^2. No flux boundaries are assumed at the outer (left and right, or top and bottom) chamber walls. An equation equivalent to eq. (S12) is needed for the species transport in the second compartment. Note that the concentration of the same species in the two compartments is not equal ($c_{s,r_1}(t) \neq c_{s,r_2}(t)$) as the membrane is providing a resistance to the transport. However, the difference is small.

Efficiency definition

The solar-to-hydrogen (STH) conversion efficiency, η, for solar water splitting at standard temperature and pressure of H_2 and O_2 is given by[7,8]:

$$\eta = \frac{1.23\ (\mathrm{V}) \cdot i_{\mathrm{operational}}\ (\mathrm{A\ m^{-2}})}{P_{\mathrm{solar}}\ (\mathrm{W\ m^{-2}})} \tag{S13}$$

Implementation and results

As mentioned before, we used the detailed balance limit to obtain the current-voltage characteristics of the two particle types with a given bandgap each, assuming perfect absorption by the particle and a transparent solution. The mediator was chosen to be the Fe^{3+}/Fe^{2+} redox couple. These characteristics (see solid curves in Figure S2) were then compared to the species-dependent load curves from the electrochemical load given by:

$$V_{\mathrm{OER}}(i_{\mathrm{photo,OER}}) = E_{\mathrm{OER}} - E_{\mathrm{Me^{++}/Me^{+}}} + \eta_{\mathrm{OER}}(i_{\mathrm{elec,OER}}) - \eta_{\mathrm{med,red}}(i_{\mathrm{elec,OER}}) + i_{\mathrm{elec,OER}} \cdot {}^{1}/_{\sigma_\mathrm{l}} \cdot l_\mathrm{i} \tag{S14}$$

$$V_{\mathrm{HER}}(i_{\mathrm{photo,HER}}) = E_{\mathrm{Me^{++}/Me^{+}}} - E_{\mathrm{HER}} + \eta_{\mathrm{med,ox}}(i_{\mathrm{elec,HER}}) - \eta_{\mathrm{HER}}(i_{\mathrm{elec,HER}}) + i_{\mathrm{elec,HER}} \cdot {}^{1}/_{\sigma_\mathrm{l}} \cdot l_\mathrm{i} \tag{S15}$$

and solved for $i_{\mathrm{photo},i} = i_{\mathrm{elec},i}$. The potential on the left-hand side indicates the potential of the particle diode, while the total potential on the right-hand side is the potential of the total electrochemical load. As can be seen in figure S2, the operating current density of the two particle types converge to the same value which represents the steady state operational current. At this point both particles produce or consume the same amount of protons and mediator ions. Thus, beyond this point the concentration profiles remain stable.

Figure S2 shows a representative simulation at a bandgap combination of 1.8 eV and 1.15 eV for a tandem HER on top configuration for a redox mediator potential of 1 V vs SHE.

We analyzed the steady state solutions in these Z-schemes for typical mediator and proton initial concentrations of 100 mol/m^3 and 1000 mol/m^3, respectively. This allowed us to map the ideal relation between the bandgap of the HER/MOR particle and the MRR/OER particle (0.6 eV – 2.4 eV) as a function of the redox equilibrium potential of the mediator (0.2 V to 1.2 V vs SHE).

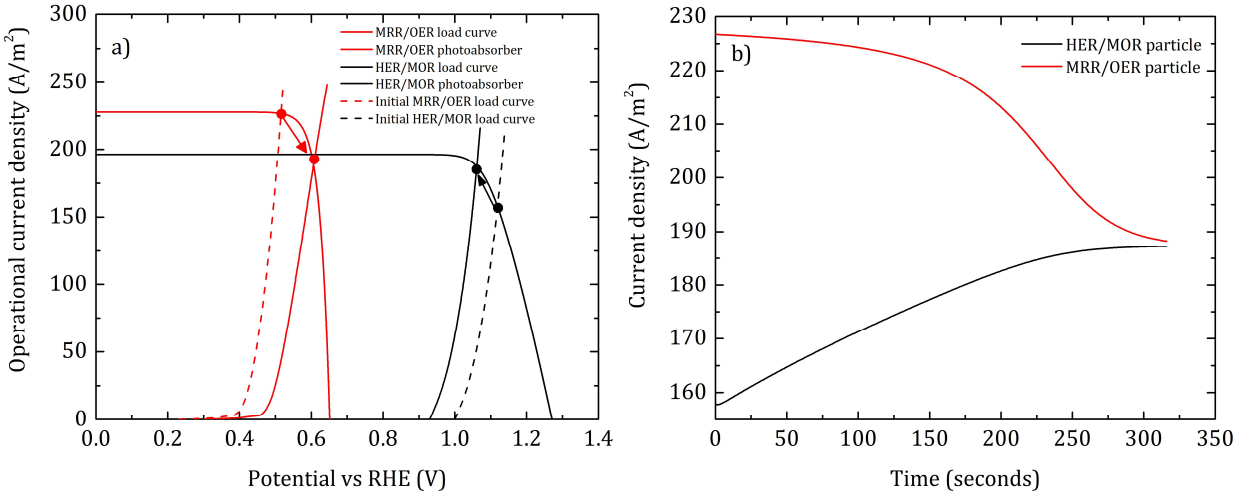

Figure S2. a) Current density versus potential of the photocatalyst and the electrochemical load for HER/MOR (black) and OER/MER (red) particle types. The dashed load curves indicate the initial operation while the corresponding second load curve indicates the steady-state operation. b) Transient evolution of the operating current density (current per projected particle area) of the two particle types.

Table S1. Reference material and kinetic parameters used in the model [7,9,10,11,12,13]

Parameter	Symbol	Value
Membrane diffusivity of H^+	$D_{\mathrm{Mem,H^+}}$	$2.4 \cdot 10^{-9}$ m^2/s
Membrane diffusivity of Fe^{2+}	$D_{\mathrm{Mem,Fe^{2+}}}$	$1.02 \cdot 10^{-9}$ m^2/s
Membrane diffusivity of Fe^{3+}	$D_{\mathrm{Mem,Fe^{3+}}}$	$7.22 \cdot 10^{-9}$ m^2/s
Ionic path length	l_{i}	10 µm
Mediator exchange current density[12]	$i_{0,\mathrm{MRR/MOR}}$	79 A/m^{-2}
Mediator transfer coefficient	$\alpha_{\mathrm{a/c,MRR/MOR}}$	0.5
Initial proton concentration	$c_{\mathrm{H^+}}$	1 mol/l
Initial mediator ion concentration	$c_{\mathrm{Me^{++}}}/c_{\mathrm{Me^+}}$	0.1 mol/l
Membrane surface	A_{Mem}	100 µm^2
Membrane thickness	t_{Mem}	500 µm
HER anodic transfer coefficient	$\alpha_{\mathrm{a,HER}}$	1
HER cathodic transfer coefficient	$\alpha_{\mathrm{c,HER}}$	1
HER exchange current density [9,11]	$i_{0,\mathrm{HER}}$	10 A/m^{-2}
OER anodic transfer coefficient	$\alpha_{\mathrm{a,OER}}$	1.7
OER cathodic transfer coefficient	$\alpha_{\mathrm{c,OER}}$	0.1
OER exchange current density [9,10]	$i_{0,\mathrm{OER}}$	$1 \cdot 10^{-4}$ A/m^{-2}

State-of-the-art catalysts and kinetic rates were chosen for the kinetic parameters[9]. Hence, kinetic values representative of Pt- and RuO_2-covered electrodes were selected for the HER and OER respectively[10]. For HER, transfer coefficients between 1 and 2 are reported[11], a value of $\alpha_{a,HER} = \alpha_{c,HER} = 1$ and for OER, $\alpha_{a,OER} = 1.7$ and $\alpha_{c,OER} = 0.1$ was used. A negligible back reaction at the potential of interest was assumed. The diffusivities in the electrolyte of protons, redox shuttle ions and counter ions were assumed to be the diffusivities of these species in water. The concentration within the electrolyte was assumed to be homogeneous. Temperature and pressure were kept under standard conditions. The particles were exposed to a constant illumination of 1000 W/m^2 for a standard AM1.5 spectrum. Table S1 summarizes the reference parameters chosen.

The modeling approach and theory remains the same for ***type 3*** with few extra requirements. Two additional overpotentials have to be considered due to the redox mediator reactions at the two wired electrodes (assumed to be described with the same kinetics as the mediator reaction at the particle, described by eq. (S7)). Two different mediators are present in the two reaction compartments. In order to maintain a Z-scheme, the equilibrium potential of the redox mediator in the HEP compartment should be more positive compared to the equilibrium potential of the redox mediator of the OEP compartment (see Figure S3). Additionally, the equilibrium potential of the redox mediator operating in the OEP compartment must be more positive than the CBM of the OEP, and the equilibrium potential of the redox mediator in HEP compartment must be more negative than VBM of the HEP.

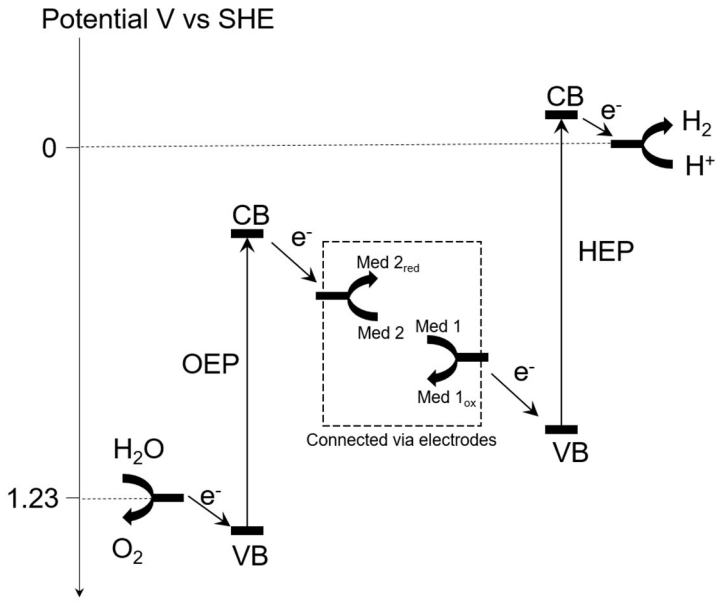

Figure S3. Energy level diagram for type 3, including valence bands (VBs), conduction bands (CBs), and reaction potentials.

References

1. Fountaine, K. T., Lewerenz, H. J. & Atwater, H. A. Interplay of light transmission and catalytic exchange current in photoelectrochemical systems. *Appl. Phys. Lett.* **105,** 173901; 10.1063/1.4900612 (2014).
2. Fountaine, K. T. & Lewerenz, H. J. (Invited) Efficiency Limits for Hydrogen and Formate Production via Fully-Integrated Photoelectrochemical Devices. *ECS Trans.* **77,** 15–23; 10.1149/07704.0015ecst (2017).
3. Shockley, W. & Queisser, H. J. Detailed Balance Limit of Efficiency of p-n Junction Solar Cells. *Journal of Applied Physics* **32,** 510–519; 10.1063/1.1736034 (1961).
4. Bockris, J. O.'M., Mannan, R. J. & Damjanovic, A. Dependence of the Rate of Electrodic Redox Reactions on the Substrate. *The Journal of Chemical Physics* **48,** 1898–1904; 10.1063/1.1668987 (1968).
5. Ban, S., Huang, C., Yuan, X.-Z. & Wang, H. Molecular simulation of gas adsorption, diffusion, and permeation in hydrated Nafion membranes. *The journal of physical chemistry. B* **115,** 11352–11358; 10.1021/jp204141b (2011).
6. Selinsek, M., Kraut, M. & Dittmeyer, R. Experimental Evaluation of a Membrane Micro Channel Reactor for Liquid Phase Direct Synthesis of Hydrogen Peroxide in Continuous Flow Using Nafion® Membranes for Safe Utilization of Undiluted Reactants. *Catalysts* **8,** 556; 10.3390/catal8110556 (2018).
7. Walter, M. G. *et al.* Solar water splitting cells. *Chemical reviews* **110,** 6446–6473; 10.1021/cr1002326 (2010).
8. Bolton, J. R., Strickler, S.J. & Connolly J.S. Limiting and realizable efficiencies of solar photolysis of water. *Nature* **316,** 495–500 (1985).
9. Haussener, S. *et al.* Modeling, simulation, and design criteria for photoelectrochemical water-splitting systems. *Energy Environ. Sci.* **5,** 9922; 10.1039/c2ee23187e (2012).
10. Trasatti, S. PII: S0022-0728(72)80485-6. *Electroanalytical Chemistry and Interfacial Electrochemistry* (1972).
11. Bockris, J. O. M., Ammar, I. A. & Huq, A. K. M. S. The Mechanism of the Hydrogen Evolution Reaction on Platinum, Silver and Tungsten surfaces in Acid Solutions. *J. Phys. Chem.* **61,** 879–886; 10.1021/j150553a008 (1957).
12. Xiong, L., Kannan, A.M. & Manthiram, A. Pt–M (M=Fe, Co, Ni and Cu) electrocatalysts synthesized by an aqueous route for proton exchange membrane fuel cells. *Electrochemistry Communications* **4,** 898–903; 10.1016/S1388-2481(02)00485-X (2002).
13. Lodi, G., Silvieri, E. & Trasatti, S. Ruthenium dioxide-based film electrodes. *Journal of Applied Electrochemistry* **8,** 135–143 (1978).